

Journal of Materials Chemistry A

Accepted Manuscript



This is an *Accepted Manuscript*, which has been through the Royal Society of Chemistry peer review process and has been accepted for publication.

Accepted Manuscripts are published online shortly after acceptance, before technical editing, formatting and proof reading. Using this free service, authors can make their results available to the community, in citable form, before we publish the edited article. We will replace this *Accepted Manuscript* with the edited and formatted *Advance Article* as soon as it is available.

You can find more information about *Accepted Manuscripts* in the [Information for Authors](#).

Please note that technical editing may introduce minor changes to the text and/or graphics, which may alter content. The journal's standard [Terms & Conditions](#) and the [Ethical guidelines](#) still apply. In no event shall the Royal Society of Chemistry be held responsible for any errors or omissions in this *Accepted Manuscript* or any consequences arising from the use of any information it contains.

COMMUNICATION

Core-shell Amorphous Cobalt Phosphide/Cadmium Sulfide Semiconductor Nanorods for Exceptional Photocatalytic Hydrogen Production under Visible Light

Cite this: DOI: 10.1039/x0xx00000x

Received 00th January 2012,
Accepted 00th January 2012

DOI: 10.1039/x0xx00000x

www.rsc.org/

Zijun Sun,^a Bihu Lv,^b Jingshi Li,^a Min Xiao,^b Xiaoyong Wang,^{*b} Pingwu Du^{*a}

Efficient hydrogen (H₂) production is considered to be a key pathway for future clean energy supply. Herein we report that a photocatalyst made of core-shell amorphous cobalt phosphide (CoP_x) integrated with cadmium sulfide nanorods (CdS NRs) gives exceptional performance of photocatalytic H₂ production under visible light. Under optimal conditions, the CoP_x/CdS NRs photocatalyst allows an H₂ evolution rate of ~500 μmol h⁻¹ mg⁻¹ based on the photocatalyst (λ > 420 nm) and the apparent quantum yield was ~35% in aqueous solution (λ = 450 nm). The turnover numbers (TONs) reached ~630000 per mole of cobalt in 70 hours with a TOF of ~9000 h⁻¹. Such high performance of an artificial photosynthetic H₂ production system using a cobalt-based cocatalyst has, to the best of our knowledge, not been reported to date.

Hydrogen is considered an ideal energy carrier for a future clean energy supply system due to its high energy capacity and environmental friendliness.^{1,2} Since the discovery of H₂ evolution through the photoelectrochemical splitting of water on TiO₂ electrodes,³ development of efficient and low-cost semiconductor photocatalysts for H₂ production from water splitting using solar energy has become a great challenge whose solution may meet future energy demands. Up to now, various semiconductors have been intensively investigated as photocatalysts for H₂ production, such as doped-TiO₂,^{4,5} g-C₃N₄,⁶ SrTiO₃,⁷ and CdSe.⁸ Cadmium sulfide (CdS), due to its desirable valence and conduction bands, is considered to be one of the promising candidates for visible light driven photocatalytic water splitting.⁹⁻¹² However, CdS alone exhibited low photocatalytic activity and stability due to its fast electron-hole recombination and photocorrosion.¹³ In most work reported so far, loading a cocatalyst on the surface of the photocatalyst plays a very important role in promoting the catalytic activity.¹⁴⁻¹⁶ An appropriate cocatalyst helps to promote charge separation, which subsequently reduces both bulk and surface

recombination of photoexcited charge carriers. By introducing noble metal cocatalysts onto the surface of semiconductors, such as Pt¹⁵ and Pd,¹⁷ the photocatalytic activity can be highly enhanced. When considering the possible commercial application, it is necessary to develop more cost-effective and robust catalysts.^{18,19}

In the past decade, cobalt-based materials have been widely investigated as noble-metal-free cocatalysts to promote photocatalytic activities of a semiconductor, such as cobalt sulfide,²⁰ cobalt hydroxide,²¹ and cobalt-based molecular catalysts (cobaloximes, cobalt dithiolenes, etc).^{22,23} However, highly efficient cocatalyst for photocatalytic H₂ production is still highly demanded for practical applications. Recently, crystalline metal phosphides were reported as highly active catalysts for electrocatalytic hydrogen evolution reaction (HER)²⁴⁻²⁶ and photocatalytic hydrogen production.²⁷⁻²⁹ Besides their impressive advances in HER, the practical implementation of these materials might be hindered by their complicated and high temperature preparation procedures. Amorphous materials are generally prepared under a mild temperature with faster solidification processes than crystalline materials, which also showed comparable activity to crystalline materials.^{30,31} Therefore, it would be of great interest to use amorphous metal phosphide prepared in a facile processes under a mild temperature for photocatalytic hydrogen evolution. To the best of our knowledge, there has no report investigating amorphous metal phosphide for photocatalytic hydrogen generation.

Herein, we report the in-situ preparation of a novel core-shell amorphous CoP_x/CdS nanorods (NRs) photocatalyst for H₂ production under visible light. Under optimal conditions, the H₂ evolution rate was as high as ~500 μmol h⁻¹ mg⁻¹ (λ > 420 nm) and the apparent quantum yield was ~35% (λ = 450 nm). The TONs reached ~630000 based on per mole of cobalt in 70 hours with a TOF of ~9000 h⁻¹. Hence, the result shows that the amorphous CoP_x cocatalyst has high photocatalytic H₂ evolution activity and stability and can serve as an excellent alternative to noble metals.

Core-shell CoP_x-modified CdS NRs were synthesized by a simple solvothermal method. The as-prepared samples were labeled

SC1, SC2, SC3, SC4, and SC5, respectively, for $\text{Co}(\text{NO}_3)_2 \cdot 6\text{H}_2\text{O}$ content 4 mg, 16 mg, 32 mg, 64 mg, and 108 mg. The real cobalt ratio in each sample was measured by ICP-AES and is shown in Table S1. The next step was to examine the photocatalytic ability of these samples.

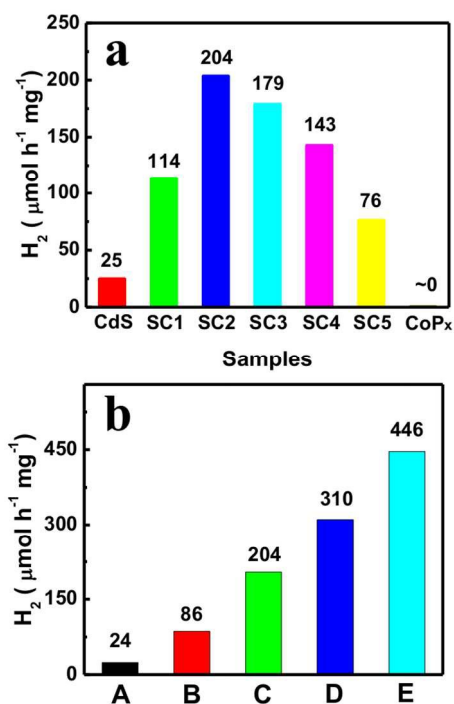


Figure 1. (a) Comparison of the photocatalytic H_2 evolution rates of the CdS, SC1, SC2, SC3, SC4, SC5, and CoPx samples under visible light ($\lambda > 420$ nm). (b) The rate of H_2 evolution for the SC2 sample under different concentrations of the hole scavenger ($\text{Na}_2\text{S}/\text{Na}_2\text{SO}_3$) under visible light ($\lambda > 420$ nm): (A) 0.25 M/0.35 M; (B) 0.5 M/0.7 M; (C) 0.75 M/1.05 M; (D) 1.25 M/1.75 M; (E) 1.5 M/2.1 M. The system contains 1 mg SC2 in 20 mL aqueous solution.

Photocatalytic H_2 evolution activity of the core-shell CoP_x/CdS NRs was evaluated under visible light irradiation ($\lambda > 420$ nm) by using $\text{Na}_2\text{S}/\text{Na}_2\text{SO}_3$ as the electron donors (Figure 1a). No appreciable H_2 was detected using only CoP_x material for irradiation. In-situ growth of CoP_x on CdS NRs significantly enhances the photocatalytic activity. Sample SC1 with 0.08% Co exhibited a H_2 evolution rate of $\sim 114 \mu\text{mol h}^{-1} \text{mg}^{-1}$, which is much higher than that of pure CdS NRs ($\sim 25 \mu\text{mol h}^{-1} \text{mg}^{-1}$). The highest photocatalytic activity was achieved using sample SC2 as the photocatalyst, with a rate of $\sim 204 \mu\text{mol h}^{-1} \text{mg}^{-1}$. Obvious H_2 bubbles were observed during photocatalysis, as seen in supplementary movie S1. Subsequent increasing content of CoP_x decreased the photocatalytic activity and the H_2 evolution rate was reduced to $\sim 76 \mu\text{mol h}^{-1} \text{mg}^{-1}$ for sample SC5. An optimum loading of a cocatalyst to produce the maximum activity has been reported in many semiconductor-cocatalyst systems.³²⁻³⁴ And this phenomenon can be explained as follows: (1) initially, more CoP_x cocatalyst provides catalytic active sites to facilitate photocatalytic H_2 production before it reaches maximum activity; (2) thereafter, excess CoP_x covered on the CdS surface can inhibit the incident light absorption of CdS, leading to decreasing the number of photogenerated electrons; (3) excess CoP_x will also merge together and reduce the catalytic active sites on the surface.^{32, 35, 36} It is well known that platinum function as efficient

hydrogen production promoters for many semiconductors. We further measured the hydrogen production activity of 0.5 wt% Pt/CdS NRs for comparison under the same conditions (Figure S1). The results show that the rate of 0.5 wt% Pt/CdS NRs is $\sim 167 \mu\text{mol h}^{-1} \text{mg}^{-1}$, which is less than SC2 samples, indicating that CoP_x is an excellent cocatalyst for hydrogen production in the present system. Figure 1b shows the effect of electron donors on the photocatalytic activity of sample SC2 for photocatalytic H_2 evolution. When increasing the concentration of $\text{Na}_2\text{S}/\text{Na}_2\text{SO}_3$ from 0.25 M/0.35 M to 1.5 M/2.1 M, a substantial increase of the amount of H_2 was observed. The results indicated that a higher concentration of electron donors probably led to faster transfer of the photogenerated holes and suppressed the electron-hole recombination.

Figure 2a displays the XRD patterns of the CdS NRs, CoP_x , and samples SC1-SC5. The hexagonal structure of CdS (PDF#77-2306) was clearly observed for CdS NRs and all the SC1-SC5 samples. The peaks located at $2\theta = 24.8^\circ, 26.5^\circ, 28.2^\circ, 36.7^\circ, 43.7^\circ, 47.9^\circ, 51.9^\circ,$ and 66.8° correspond to the (100), (002), (101), (102), (110), (103), (112), and (203) planes, respectively.³⁷ No obvious crystalline cobalt phosphide peak was observed in any of these samples. Moreover, the XRD diffraction pattern of pure CoP_x showed no diffraction peaks, which probably indicates that the CoP_x had amorphous structure.

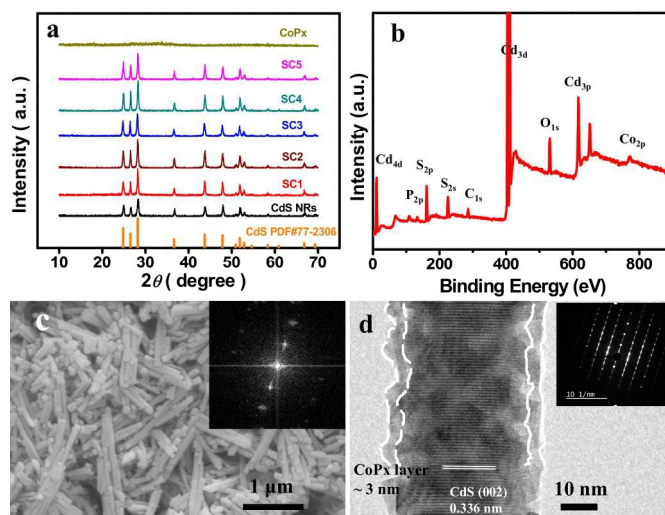


Figure 2. (a) XRD patterns of the CdS, SC1, SC2, SC3, SC4, SC5, and CoP_x samples. (b) XPS data, (c) SEM image, (d) HRTEM image of SC2 sample. (Insert of (c), FFT of HRTEM image; inset of (d), SAED of SC2 sample).

The XPS spectra (Figure 2b and Figure S2) of the SC2 sample showed the existence of Cd, S, Co, and P elements and their XPS peaks appeared at binding energies of 404.6 eV (Cd 3d), 161.2 eV (S 2p), 780.5 eV (Co 2p), and 133.5 eV (P 2p). No other elements were observed except C element as the reference and O element from the absorbed gaseous molecules. The binding energy of Cd 3d and S 2p was in agreement with the CdS.³⁸ The XPS spectra of pure CoP_x are showed in Figure S3 for comparison. The binding energy of Co 2p showed that the cobalt was in the oxidation state^{39, 40} and no metallic cobalt was formed. For P 2p, pure CoP_x showed two peaks at 129.9 eV and 133.5 eV, respectively. The former one is probably contributed to the formation of cobalt phosphide, while latter one can be assigned to phosphate species. However, due to the very low content of cobalt phosphide in SC2 sample, only strong peak at

133.5 eV was observed, which may come from the solvothermal synthesis process under the phosphorus-rich conditions. The SEM image (Figure 2c) shows the morphology of CoP_x/CdS NRs photocatalyst, indicating an average diameter of 40-90 nm and the length of 0.5-1.5 μm . Comparing to the pure CdS NRs (Figure S4a), the nanorods in sample SC2 became thicker with a larger diameter. In addition, pure CoP_x showed no specific shape and obvious irregular particles were observed (Figure S4b).

A fast Fourier transform (FFT) of the HRTEM image showed diffuse rings and ordered diffraction spots (inset of Figure 2c), which suggests that the amorphous CoP_x was successfully deposited on the surface of crystalline CdS NRs. The HRTEM image clearly shows the core-shell structure of sample SC2 (Figure 2d), further confirming that the CoP_x was successfully loaded onto the CdS NRs. The distance between ordered lattice planes of 0.67 nm can be assigned to the (002) plane of crystal hexagonal CdS.³⁷ In addition, the selected-area electron diffraction (SAED) analysis (inset of Figure 2d) showed the sample mainly contained single crystal CdS NRs.

Moreover, the EDX data (Figure 3a) confirmed the existence and distribution of Co, P, Cd, and S elements, as well as C as the reference and O from the absorbed gaseous molecules. Cu element is from the copper grid substrate. The EDX-mapping images of a single nanorod show that Co and P are uniformly distributed over the whole surface of the rod, demonstrating that amorphous CoP_x was tightly deposited onto the surface of the CdS NRs.

The apparent quantum yield (ϕ) for photocatalytic H_2 production under visible light was measured using an excitation at 450 nm (± 5 nm) (Figure 4a). The result showed that the H_2 evolution rate was $\sim 120 \mu\text{mol h}^{-1} \text{mg}^{-1}$ with $\phi > 35\%$ after 3 hours, although there was a slightly lower rate of $\sim 60 \mu\text{mol h}^{-1} \text{mg}^{-1}$ in the first hour ($\phi \sim 17\%$). The results indicated that CoP_x/CdS NRs is an exceptional photocatalyst for electron-hole pair generation and separation and subsequent photocatalytic H_2 production.

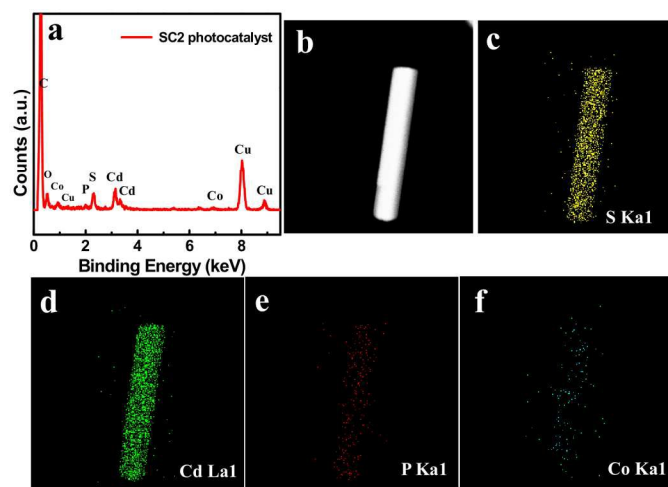


Figure 3. (a) EDX and EDX-mapping of SC2 sample: (b) bright field image, (c) S mapping, (d) Cd mapping, (e) P mapping, and (f) Co mapping.

To reveal the durability of the CoP_x/CdS photocatalyst, long-term irradiation under visible light was performed. A total of ~ 35 mmol H_2 was produced within 70 h of irradiation (Figure 4b), corresponding to ~ 630000 turnover numbers (TONs) and $\sim 9000 \text{ h}^{-1}$ turnover frequency (TOF) with respect to the cobalt. The H_2 evolution rate reached $\sim 500 \mu\text{mol h}^{-1} \text{mg}^{-1}$ and the activity was

maintained without noticeable decrease during the illumination for 70 h. The CoP_x cocatalyst has exceptional photocatalytic H_2 evolution activity and is superior to any other cobalt-based cocatalysts reported in the literature, like CoO_x ($660 \mu\text{mol h}^{-1} \text{g}^{-1}$, TOF ~ 2 moles of H_2 per mole of per mole cobalt per hour),³⁸ CoS_x ($0.84 \mu\text{mol h}^{-1} \text{mg}^{-1}$),²⁰ $\text{Co}(\text{OH})_2$ ($61 \mu\text{mol h}^{-1} \text{g}^{-1}$),²¹ cobalt dithiolene complex (TONs > 300000 in 60 h, TOF $> 5500 \text{ h}^{-1}$),^{23, 41} and inorganic cobalt salts ($25 \mu\text{mol h}^{-1} \text{mg}^{-1}$, TONs ~ 59600 moles of H_2 , and TOF ~ 1114 moles of H_2 per hour of per moles cobalt).⁴² Amorphous CoP_x cocatalyst therefore represent an important addition to greatly enrich our knowledge and shows the exceptional H_2 evolution activity about the growing family of Co-based photocatalytic cocatalysts.

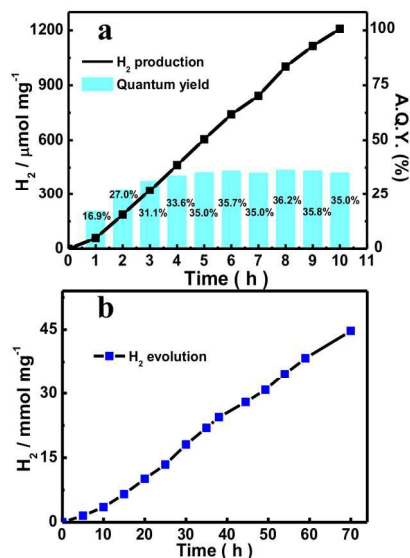


Figure 4. (a) Time courses of H_2 evolution and apparent quantum yield on SC2 (b) Long-term H_2 evolution on SC2.

Figure S5 shows the H_2 evolution curve in cycling photocatalytic runs. The results indicate that the photocatalyst did not display any obvious decrease of H_2 production activity. Moreover, sample SC2 had similar morphology before and after irradiation, as seen by SEM images (Figure S4a and Figure S6). The high-resolution XPS spectrum of Co 2p (Figure S7a) showed no obvious changes and no metallic Co was detected after irradiation, suggesting that CoP_x does not decompose to produce Co(0) during the photocatalytic H_2 evolution reaction. As for P 2p (Figure S7b), it is observed that the peak at 133.5 eV disappeared during the photocatalytic hydrogen evolution, indicating that phosphate species is not the active sites and can be dissolved during the photocatalytic hydrogen evolution.

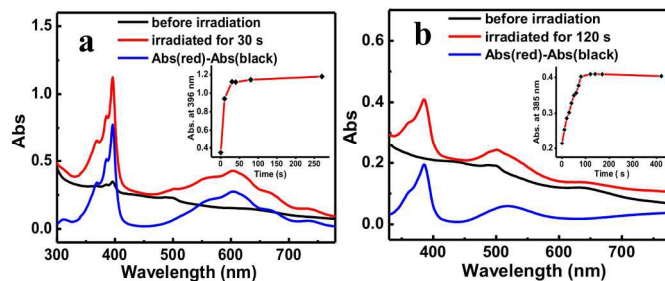


Figure 5. UV-vis absorption spectra of (a) MV^{2+} and (b) DQ^{2+} using SC2 sample. (Inset image: time course of absorption changes of (a) MV^{2+} at 396 nm and (b) DQ^{2+} at 385 nm). Condition: a 3 mL aqueous solution containing sample SC2 ($8.3 \mu\text{g}\cdot\text{mL}^{-1}$), 0.625 M Na_2S and 0.875 M Na_2SO_3 and 3×10^{-5} M MV^{2+} (or DQ^{2+}) were filled with N_2 and irradiated under visible light using 300 W Xe lamp ($\lambda > 420$ nm).

The reducing power of the CoP_x/CdS NRs was investigated by using organic electron acceptors.²³ When the SC2 sample in $\text{Na}_2\text{S}/\text{Na}_2\text{SO}_3$ solution was irradiated in the presence of methyl viologen dication (MV^{2+}) as electron acceptor, the color rapidly changed from yellow to blue and its absorption intensity was saturated within only one minute, indicating a fast electron transfer and the formation of reduced MV^{+} (Figure 5a).⁴³ A diquat acceptor, DQ^{2+} (N,N'-(1,3-propylene)-5,5'-dimethylbipyridine), was also used as the electron acceptor for irradiation. The result also showed a rapid color change from yellow to pink, indicating the formation of DQ^{+} (Figure 5b).⁴³ Considering DQ^{2+} reduction potential is ~ 0.7 V vs. NHE,²³ the above result suggested that the reducing ability of CoP_x/CdS NRs corresponds to a potential more negative than -0.7 V vs. NHE, and thus the excited state is sufficiently reducing for H^+ reduction.

A possible reaction mechanism is proposed for CoP_x/CdS NRs to enhance photocatalytic activity. Under visible light irradiation, the semiconductor CdS NRs absorb photons and generate electron-hole pairs. Without loading a cocatalyst, the photogenerated electrons and holes are likely to be recombined together, resulting in low catalytic activity. After loading CoP_x cocatalyst, the close contact interfaces between CoP_x and CdS NRs are formed. Photogenerated electrons in the conduction band of CdS NRs can be quickly transferred to CoP_x cocatalysts via contacting interfaces, resulting in great improvement of photocatalytic H_2 evolution for the CoP_x/CdS NRs photocatalyst.

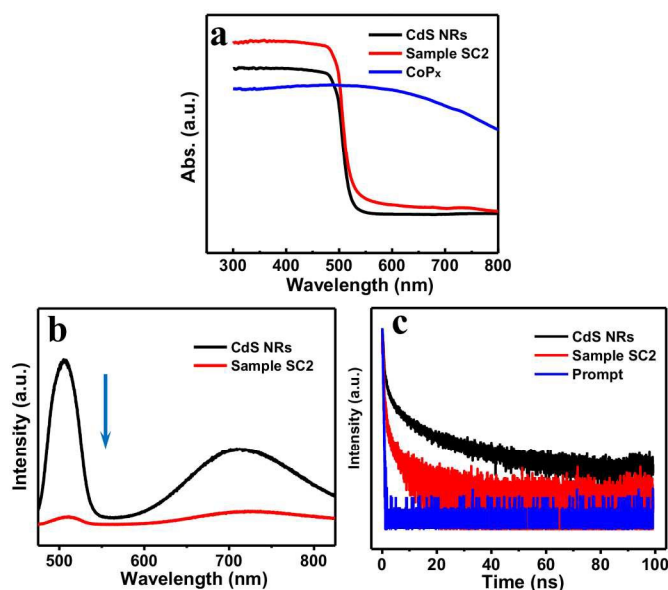


Figure 6. (a) UV-vis diffuse reflectance spectra of CdS NRs, SC2 sample, and CoP_x . (b) Photoluminescence (PL) spectra and (c) Time-resolved photoluminescence (TRPL) spectra of CdS NRs and SC2 sample with an excitation wavelength of 405 nm.

To verify the above analysis, the UV-vis, photoluminescence (PL), and time-resolved photoluminescence (TRPL) spectra were performed. No appreciable shift of the absorption edge was observed for CdS and CoP_x/CdS (Figure 6a). Under an excitation wavelength of 405 nm, the PL intensity maximized at ~ 511 nm and ~ 713 nm obtained for sample SC2 was much weaker than that of CdS NRs (Figure 6b), suggesting a much faster charge transfer process occurred from CdS NRs to CoP_x shell. The more efficient transfer of photogenerated charge carriers in CoP_x/CdS NRs than that in pure CdS NRs was also confirmed by TRPL spectra (Figure 6c). The lifetime of sample SC2 was much shorter than that of CdS NRs. The CdS NRs material had two decay time values: 503 ps and 7.74 ns. The short lifetime component is attributed to quasi-free excitons,⁴⁴ which are rapidly trapped by the surface states. The long component is attributed to localized exciton recombination, which is caused by de-trapping of carriers. Only one decay lifetime value at ~ 411 ps was observed in SC2. The significant decrease of the long lifetime indicated faster charge transfer from CdS to amorphous CoP_x , revealing that CoP_x is an effective cocatalyst for photocatalytic H_2 production.

Conclusions

In conclusion, we developed a simple solvothermal method to synthesize a core-shell heterostructure of amorphous CoP_x integrated with CdS NRs for photocatalytic H_2 evolution under visible light. The results demonstrated that the amorphous cobalt phosphide is a highly efficient cocatalyst to enhance the photocatalytic H_2 production activity and durability by promoting the photoinduced charge transfer process and suppressing the electron-hole recombination. The work also showed that amorphous CoP_x , which is made of earth-abundant elements, could serve as an important substitute for precious platinum for photocatalytic H_2 production.

Acknowledgements

This work was financially supported by NSFC (21271166, 21473170), the Fundamental Research Funds for the Central Universities (WK3430000001, WK2060140015, WK2060190026), the Program for New Century Excellent Talents in University (NCET), and the Thousand Young Talents Program.

Notes and references

- ^a Key Laboratory of Materials for Energy Conversion, Chinese Academy of Sciences, Department of Materials Science and Engineering, iChEM (Collaborative Innovation Center of Chemistry for Energy Materials), University of Science and Technology of China, 96 Jinzhai Road, Hefei, Anhui Province, 230026, P. R. China. Fax: 86-551-63606207; E-mail: dupingwu@ustc.edu.cn
- ^b National Laboratory of Solid State Microstructures and School of Physics, Nanjing University, Nanjing, Jiangsu Province, 210093, P. R. China. E-mail: wxiaoyong@nju.edu.cn

†Electronic Supplementary Information (ESI) available: Experimental details, ICP-AES results, SEM images of CdS NRs and CoP_x , and XPS data for sample SC2 before and after photocatalytic hydrogen production under visible light. See DOI: 10.1039/c000000x/

1. H. B. Gray, *Nat. Chem.*, 2009, **1**, 7-7.
2. N. S. Lewis and D. G. Nocera, *Proc. Natl. Acad. Sci. U. S. A.*, 2006, **103**, 15729-15735.
3. A. Fujishima and K. Honda, *Nature*, 1972, **238**, 37-38.

4. T. Ohno, T. Mitsui and M. Matsumura, *Chem. Lett.*, 2003, **32**, 364-365.
5. J. Wang, D. N. Tafen, J. P. Lewis, Z. L. Hong, A. Manivannan, M. J. Zhi, M. Li and N. Q. Wu, *J. Am. Chem. Soc.*, 2009, **131**, 12290-12297.
6. X. C. Wang, K. Maeda, A. Thomas, K. Takanabe, G. Xin, J. M. Carlsson, K. Domen and M. Antonietti, *Nat. Mater.*, 2009, **8**, 76-80.
7. M. Miyauchi, M. Takashio and H. Tobimatsu, *Langmuir*, 2004, **20**, 232-236.
8. C. Harris and P. V. Kamat, *ACS Nano*, 2009, **3**, 682-690.
9. M. Matsumura, S. Furukawa, Y. Saho and H. Tsubomura, *J. Phys. Chem.*, 1985, **89**, 1327-1329.
10. J. F. Reber and M. Rusek, *J. Phys. Chem.*, 1986, **90**, 824-834.
11. Q. Z. Wang, J. J. Li, Y. Bai, J. H. Lian, H. H. Huang, Z. M. Li, Z. Q. Lei and W. F. Shangguan, *Green Chem.*, 2014, **16**, 2728-2735.
12. Q. Z. Wang, J. H. Lian, J. J. Li, R. F. Wang, H. H. Huang, B. T. Su and Z. Q. Lei, *Sci. Rep.*, 2015, **5**, 13593.
13. A. Kudo and Y. Miseki, *Chem. Soc. Rev.*, 2009, **38**, 253-278.
14. K. Maeda, A. K. Xiong, T. Yoshinaga, T. Ikeda, N. Sakamoto, T. Hisatomi, M. Takashima, D. L. Lu, M. Kanehara, T. Setoyama, T. Teranishi and K. Domen, *Angew. Chem. Int. Ed.*, 2010, **122**, 4190-4193.
15. J. H. Yang, D. G. Wang, H. X. Han and C. Li, *Acc. Chem. Res.*, 2013, **46**, 1900-1909.
16. X. Zong, H. J. Yan, G. P. Wu, G. J. Ma, F. Y. Wen, L. Wang and C. Li, *J. Am. Chem. Soc.*, 2008, **130**, 7176-7177.
17. T. Sreethawong and S. Yoshikawa, *Catal. Commun.*, 2005, **6**, 661-668.
18. P. Du and R. Eisenberg, *Energy Environ. Sci.*, 2012, **5**, 6012-6021.
19. D. G. Nocera, *Acc. Chem. Res.*, 2012, **45**, 767-776.
20. Z. M. Yu, J. L. Meng, J. R. Xiao, Y. Li and Y. D. Li, *Int. J. Hydrogen Energy*, 2014, **39**, 15387-15393.
21. L. J. Zhang, R. Zheng, S. Li, B. K. Liu, D. J. Wang, L. L. Wang and T. F. Xie, *ACS Appl. Mater. Interfaces*, 2014, **6**, 13406-13412.
22. P. W. Du, K. Knowles and R. Eisenberg, *J. Am. Chem. Soc.*, 2008, **130**, 12576-12577.
23. A. Das, Z. Han, M. G. Haghghi and R. Eisenberg, *Proc. Natl. Acad. Sci. U. S. A.*, 2013, **110**, 16716-16723.
24. H. F. Du, Q. Liu, N. Y. Cheng, A. M. Asiri, X. P. Sun and C. M. Li, *J. Mater. Chem. A*, 2014, **2**, 14812-14816.
25. J. Q. Tian, Q. Liu, A. M. Asiri and X. P. Sun, *J. Am. Chem. Soc.*, 2014, **136**, 7587-7590.
26. E. J. Popczun, C. G. Read, C. W. Roske, N. S. Lewis and R. E. Schaak, *Angew. Chem. Int. Ed.*, 2014, **126**, 5531-5534.
27. Z. Sun, H. Zheng, J. Li and P. Du, *Energy Environ. Sci.*, 2015, 2668-2676.
28. Q. Yue, Y. Wan, Z. Sun, X. Wu, Y. Yuan and P. Du, *J. Mater. Chem. A*, 2015, 16941-16947.
29. Z. Sun, Q. Yue, J. Li, J. Xu, H. Zheng and P. Du, *J. Mater. Chem. A*, 2015, 10243-10247.
30. D. Merki, S. Fierro, H. Vrubel and X. L. Hu, *Chem. Sci.*, 2011, **2**, 1262-1267.
31. C. G. Morales-Guio and X. L. Hu, *Acc. Chem. Res.*, 2014, **47**, 2671-2681.
32. A. Dickinson, D. James, N. Perkins, T. Cassidy and M. Bowker, *J. Mol. Catal. A: Chem.*, 1999, **146**, 211-221.
33. M. Hara, J. Nunoshige, T. Takata, J. N. Kondo and K. Domen, *Chem. Commun.*, 2003, 3000-3001.
34. X. Zong, H. J. Yan, G. P. Wu, G. J. Ma, F. Y. Wen, L. Wang and C. Li, *J. Am. Chem. Soc.*, 2008, **130**, 7176-7177.
35. J. G. Hou, C. Yang, Z. Wang, S. Q. Jiao and H. M. Zhu, *RSC Adv.*, 2012, **2**, 10330-10336.
36. J. Zhang, S. Z. Qiao, L. F. Qi and J. G. Yu, *Phys. Chem. Chem. Phys.*, 2013, **15**, 12088-12094.
37. J. S. Jang, U. A. Joshi and J. S. Lee, *J. Phys. Chem. C*, 2007, **111**, 13280-13287.
38. Z. P. Yan, X. X. Yu, A. Han, P. Xu and P. W. Du, *J. Phys. Chem. C*, 2014, **118**, 22896-22903.
39. T. J. Chuang, C. R. Brundle and D. W. Rice, *Surf. Sci.*, 1976, **59**, 413-429.
40. Y. Okamoto, T. Imanaka and S. Teranishi, *J. Catal.*, 1980, **65**, 448-460.
41. W. R. McNamara, Z. Han, P. J. Alperin, W. W. Brennessel, P. L. Holland and R. Eisenberg, *J. Am. Chem. Soc.*, 2011, **133**, 15368-15371.
42. Z. J. Li, X. B. Li, J. J. Wang, S. Yu, C. B. Li, C. H. Tung and L. Z. Wu, *Energy Environ. Sci.*, 2013, **6**, 465-469.
43. P. Du, J. Schneider, P. Jarosz, J. Zhang, W. W. Brennessel and R. Eisenberg, *J. Phys. Chem. B*, 2007, **111**, 6887-6894.
44. G. H. Ma, S. H. Tang, W. X. Sun, Z. X. Shen, W. M. Huang and J. L. Shi, *Phys. Lett. A*, 2002, **299**, 581-585.

TOC Figure

Herein we report that a photocatalyst made of core-shell amorphous cobalt phosphide (CoP_x) integrated with CdS NRs for H₂ production under visible light. The CoP_x/CdS NRs gave an H₂ evolution rate of ~500 μmol h⁻¹ mg⁻¹ based on the photocatalyst (λ > 420 nm) and the apparent quantum yield was ~35% in aqueous solution (λ = 450 nm).

